Environmental and Climate Technologies
2026, vol. 30, no. 1, pp. 495–510
https://doi.org/10.2478/rtuect-2026-0034
https://content.sciendo.com

Response Surface-Based Optimization of Single-Cell Protein Production in *Phaffia rhodozyma*

Zane KUSNERE[1]*, Svetlana RAITA[2], Iveta KUZMIKA[3], Jelizaveta PALCEVSKA[4], Zane GEIBA[5], Taras MIKA[6], Karlis VALTERS[7]

[1–7]*Institute of Energy Systems and Environment, Riga Technical University, Azenes iela 12/1, Riga, LV-1048, Latvia*

Received 04.03.2026; accepted 23.09.2026

***Abstract* – The yeast *Phaffia rhodozyma* is widely used as a natural source of astaxanthin for aquaculture, but its protein-rich biomass has been less studied as single-cell protein (SCP). This study explored the potential of *P. rhodozyma* as a dual-purpose production system by optimizing a low-cost medium for a protein-enriched mutant (AEC3/9), while also monitoring astaxanthin formation. A central composite design and response surface methodology (RSM) were used to evaluate the effects of glycerol, urea, ammonium sulphate, and initial pH. Shake-flask cultivations performed in triplicate (250 mL baffled flasks, 20 mL working volume, 22 °C, 250 rpm, 7 days) showed that protein productivity reached its maximum on day 4, which was selected as the reference point for optimization. Astaxanthin was included in the model but was not used as the main optimization target. The optimization results suggested that moderate glycerol concentrations (70–90 g/L), low urea (<0.2 g/L), and slightly acidic pH (5.9) were the most suitable conditions. Under the selected conditions (70.54 g/L glycerol, 0.134 g/L urea, 4.98 g/L $(NH_4)_2SO_4$, pH 5.86), biomass reached 26.11 g/L with a protein content of 29.79 % (7.78 g/L). Scale-up in a 5 L stirred-tank bioreactor confirmed the feasibility of the process, reaching 33.50 g/L biomass and 6.82 g/L protein at 88 h. The results indicate that protein accumulation occurs before the phase associated with increased astaxanthin production. Optimizing nitrogen source and pH allows stable production of *P. rhodozyma* biomass on glycerol, supporting its use as an SCP co-product alongside astaxanthin.**

***Keywords* – Astaxanthin co-production; effective substrate conversion; fermentation optimization; scale-up; single-cell protein.**

1. INTRODUCTION

Single-cell proteins (SCPs) refer to microbial biomass produced from various microorganisms such as yeasts, filamentous fungi, bacteria, photosynthetic microalgae, and

* Corresponding author.
E-mail address: Zane.Kusnere@rtu.lv

Zane KUSNERE https://orcid.org/0000-0002-0596-5413
Svetlana RAITA https://orcid.org/0000-0003-1899-9687
Iveta KUZMIKA https://orcid.org/0009-0009-9775-6472
Jelizaveta PALCEVSKA https://orcid.org/0009-0006-9489-7235
Zane GEIBA https://orcid.org/0009-0007-6157-6897
Taras MIKA https://orcid.org/0009-0000-2865-782X
Karlis VALTERS https://orcid.org/0000-0002-7319-2862

©2026 Author(s). This is an open access article licensed under the Creative Commons Attribution License (http://creativecommons.org/licenses/by/4.0).

cyanobacteria. Their growing relevance in biotechnology is driven by the ability to produce high-value protein-rich biomass through efficient, scalable, and sustainable cultivation systems that require minimal land, energy, and nutrient inputs. This makes SCPs a promising alternative to conventional protein sources in both food and feed applications, particularly in the context of global protein demand and environmental constraints [1].

Beyond their macronutrient contribution, SCPs are known to contain bioactive and immuno-stimulating compounds, which can provide additional functional benefits in animal nutrition [2], [3]. Yeast-based SCPs, such as *Candida utilis*, have been shown to prevent soybean meal-induced enteropathy in Atlantic salmon when included at 200 g/kg in the diet [4]. One of the frequently cited limitations in the application of single-cell proteins (SCPs) is their relatively high nucleic acid content, typically 7–12 % in fungal biomass, which exceeds the levels found in conventional protein sources such as fishmeal or plant-derived meals (<1.3 %) [5]–[8]. The limited enzymatic degradation of nucleic acids in mammals makes them more sensitive to high levels in the diet. In contrast, fish have high activity of the enzyme urate oxidase (uricase), which allows them to catabolise high concentrations of nucleic acids [3], [5]. Atlantic salmon can digest bacterial biomass of 360 g/kg of feed weight, which accounts for 39.96 g of nucleic acids, without negative effects on health [5], [9]. It can be assumed that the amount of yeast biomass added to fish feed to replace fishmeal successfully depends on the final concentration of nucleic acids in the feed. Several studies indicate that the acceptable threshold concentration of nucleic acids is close to 5–10 % in finished fish feed [10], [11].

Despite the biological suitability of SCPs for aquaculture feed, the cost of production remains a major barrier to SCP commercialization, largely due to the high price of complex organic nitrogen sources like peptones and yeast extract. Therefore, medium optimization to enable the replacement of these components with inexpensive alternatives, such as inorganic nitrogen salts and agro-industrial by-products, is essential for improving economic feasibility. Response surface methodology (RSM) is a well-established statistical and mathematical approach commonly used to optimize fermentation media and cultivation parameters in microbial bioprocesses, including the production of protein, lipid, astaxanthin, bioethanol, and enzymes [12]–[16]. Its application is particularly relevant in systems utilizing agro-industrial by-products as fermentation substrates, where process optimization is essential to improve yield, reduce costs, and enhance overall process efficiency. RSM facilitates experimental design, model generation, and quantitative analysis of the effects of multiple variables on one or more response factors [17].

The present study focuses on optimizing the glycerol-salt-based medium for the cultivation of mutant strain of *Phaffia rhodozyma* for SCP production. The mutant strain *P. rhodozyma* AEC3/9 has demonstrated enhanced protein quality in prior research, characterized by elevated levels of essential amino acids such as lysine, methionine, phenylalanine, and isoleucine when grown in a nutrient-rich medium [18]. However, the high cost of complex nitrogen sources, particularly peptones and yeast extract, remains a key barrier to the economic viability of SCP. To address this limitation, 90 % of the organic nitrogen components were replaced with inorganic nitrogen sources, aiming to develop a low-cost, scalable fermentation medium. This study applied RSM based on a central composite design (CCD), a statistically robust and widely adopted experimental approach that enables comprehensive evaluation of factor interactions, accurate modelling of response surface curvature, and reliable estimation of experimental error.

Building on this design, cultivation experiments were performed to evaluate the individual and interactive effects of glycerol, ammonium sulphate, urea, and initial pH, with each factor tested at five levels to model their influence on biomass and protein production. For medium

optimization, biomass yield and protein content were selected as key response variables. Based on model predictions, several medium formulations were proposed and validated in follow-up flask experiments. These results highlight the potential of *P. rhodozyma* as a dual-purpose microorganism for economically viable SCP production, combining efficient biomass generation with the co-production of astaxanthin, a commercially important carotenoid for feed and nutraceutical markets.

2. MATERIALS AND METHODS

2.1. Strain and Inoculum Preparation

The mutant strain *Phaffia rhodozyma* AEC3/9 was used in this study. Prior to experimentation, fresh working cultures were maintained at 4 °C on a Yeast-Malt medium (YM) agar plate. For inoculum preparation, 20 mL of YM broth in a 50 mL conical tube was used for shake flask experiments, while eight 250 mL baffled Erlenmeyer flasks, each containing 50 mL of YM broth, were prepared for bioreactor inoculation. All cultures were incubated at 22 °C for 72 h in a rotary shaker (Elmi, DOS-20L) set at 250 rpm. For shake flask experiments, a standardized inoculum density of 1.0×10^6 cells/mL was used while bioreactor fermentations were initiated with a 10 % (v/v) inoculum.

2.2. Composition of Media

The YM medium used for inoculum preparation contained of 5 g/L peptone, 3 g/L malt extract, 3 g/L yeast extract, and 10 g/L glucose. Glucose was sterilized separately and added into medium under sterile conditions. The components of the experimental fermentation media were divided into two distinct categories: the constant and the variable. The constant components were as follows: 1 g/L yeast extract, 3.2 g/L soy peptone, and 1.7 g/L yeast nitrogen base (YNB) without amino acids. The variables were: 60–120 g/L glycerol, 0.13–2.16 g/L CH_4N_2O, and 1–9 g/L $(NH_4)_2SO_4$. The initial pH of the media was adjusted within the range of 3.0 to 7.0, depending on the experimental design. The optimized formulation of Medium 1 used in the bioreactor experiment.

2.3. Experimental Conditions

Flask experiment was designed to determine the most suitable medium for promoting *P. rhodozyma* mutant strain growth and protein production. The yeast was inoculated in triplicate into 250 mL baffled flasks with a working volume of 20 mL at an initial cell concentration of 1.0×10^6 cells/mL. Flasks were incubated for 7 days at 22 °C on a rotary shaker (Elmi, DOS-20L) at 250 rpm. Samples were collected for biomass thermogravimetric analysis, total protein and astaxanthin analysis from the 3rd day of cultivation onwards.

The batch fermentation in a 5-L stirred-type F0-BABY bioreactor (Bionet, Spain) with 4 L work volume was used to test optimized medium. Dissolved oxygen (DO) and pH were continuously controlled throughout the process to 5.86 and 70 %, respectively. For pH control, sterilized 2 M NaOH and 2 M HCl were prepared. To maintain DO at 70 %, stirring speed, aeration rate, and O_2 supply were adaptively controlled. The agitation speed ranged from 400 to 1200 rpm, the aeration rate varied from 1.3 to 16.67 slpm, and the O_2 supply ranged from 0 to 1.67 slpm. The temperature was set to 22 °C. 3.9 g/L of antifoam 204 (Sigma Aldrich, USA) was added to the fermentation medium to prevent foaming, and an additional antifoam solution (15 g/100 mL of water) was connected to the automatic pump system to regulate the amount of foam during the process. Samples were taken at 0, 16, 25, 39, 48, 65, 74, 88, 97, and 112 hours of fermentation. The biomass

samples were analysed for cell count and total protein, and the medium samples were analysed for glycerol content and C/N ratio.

2.4. Experimental Study Design Using RSM

A 4^5 factorial design (Table 1) was implemented in order to evaluate the optimal medium composition and pH for batch fermentation of *P. rhodozyma* using the response surface methodology with the central composite design (CCD). The independent variables glycerol, CH_4N_2O, $(NH_4)_2SO_4$, and medium pH were selected for optimisation, with a total of 31 runs. The dependent variables chosen were biomass concentration (g/L), protein content (%), astaxanthin content (%).

TABLE 1. TYPE SIZES, SPACES AND INTERVALS

Independent factors	Symbol	Range (g/L) and levels				
		−2	**−1**	**0**	**1**	**2**
Glycerol	A	60	75	90	105	120
CH_4N_2O	B	0.13	0.63	1.13	1.63	2.13
$(NH_4)_2SO_4$	C	1	3	5	7	9
pH	D	3	4	5	6	7

2.5. Quantitative and Qualitative Analysis of Biomass

All samples for analyses were washed with distilled water after biomass harvesting. The growth of yeast biomass in 31 variations of the media was assessed thermogravimetrically every day from the 3rd to 7th day of the experiment. Biomass was collected from 1 mL of each flask trial sample and harvested by centrifugation at 10 000 × g for 5 min at 4 °C. Then supernatant was decanted, and biomass samples were dried at 105 °C overnight until weight stabilization.

Concentrations of protein and astaxanthin in yeast biomass samples were analysed from the 3rd to 7th day of the optimization experiment for flasks, excluding samples with biomass below 2 g/L. Protein extraction from yeast biomass was performed following the protocol described by Guerlava *et al*. [19], with minor modifications. Dried cells were mechanically disrupted, and 0.01 g was suspended in 1 mL of 0.05 M 3-(N-morpholino)propanesulfonic acid (MOPS) buffer and vortexed for several minutes to initiate pre-extraction. Then, the sample was centrifuged at 16 000 × g, for 10 min at 5 °C. Following centrifugation, 900 µL of the supernatant was removed, and the pellet was resuspended in 1 mL of a solution containing 0.2 M sodium hydroxide and 2.5 % sodium dodecyl sulphate. To enhance mechanical cell disruption, approximately one micro-spoonful of 0.5 mm diameter glass beads was added. The sample was vortexed for one minute and subjected to thermal lysis by incubation in a 100 °C water bath for five minutes, followed by immediate cooling in an ice bath. An aliquot of the lysate was diluted with distilled water to a final protein concentration of approximately 750 µg/mL. Protein quantification was performed using a Bicinchoninic Acid (BCA) Assay Kit (Millipore, USA; No. 71285-3) according to the manufacturer's instructions. Absorbance was measured at 562 nm using a UV–Vis spectrophotometer (BioMate™ 160, ThermoFisher Scientific).

For astaxanthin analysis, 75 µL of yeast biomass was collected, briefly centrifuged to remove residual medium, washed twice with distilled water, and stored at –20 °C until extraction. Extraction was carried out using a modified method of Luna-Flores *et al.* [20]. Briefly, 0.5 mL of preheated dimethyl sulfoxide was added to sample, followed by vortexing

and incubation at 65 °C for 15 minutes. Afterward, 0.1 mL of 0.01 M sodium phosphate buffer (pH 7.0) and 1 mL of a 1:1 (v/v) hexane:ethyl acetate mixture were added. The samples were vortexed and centrifuged at 14 000 rpm (21 694 × g) for 5 minutes to separate the phases. The upper organic phase (600 µL) was transferred to a glass cuvette, and astaxanthin concentration was determined spectrophotometrically at 474 nm and 452 nm (BioMate™ 160, Thermo Fisher Scientific). Hexane and ethyl acetate in a 1:1 ratio was used for a blank measurement. Then astaxanthin concentration measurements were performed at two wavelengths (474 nm and 452 nm) as described in [21].

The carbon and nitrogen contents of fermentation medium samples from the bioreactor were determined using the combustion method (CNHS-O analyser, COSTECH). Glycerol was determined by liquid chromatography using an HPLC-grade glycerol >99.5 %, (Sigma-Aldrich, USA) as an external standard. For determination of glycerol content in fermentation broth – liquid part was treated with 20 % trifluor acetic acid (Sigma-Aldrich, 99 %), centrifuged for 5 min at 12 000 rpm and filtered. Chromatography was performed on Shimadzu Nexera X3 series HPLC-system equipped by refractive index detector (RID) using sugar Shodex SC1011 column (8.0 mm × 300 mm, 6 µm) operated at a temperature 85 °C (flow rate 0.6 mL/min; injection volume 20 µL, deionized water was used as a mobile phase; RID temperature 40 °C).

2.6. Data Analysis and Software

Experimental design data were processed using Stat-Ease 360 software, version 23.1.8 64-bit (Stat-Ease Inc., Minneapolis, MN, USA). Second-order polynomial models were fitted to the experimental responses, and analysis of variance (ANOVA) was performed to assess model significance. Fisher's F-test was used to determine the statistical relevance of the models, with terms considered significant at $p < 0.05$. Lack-of-fit tests were applied to verify model adequacy, and square root transformation was used where necessary to improve the normality and homogeneity of residuals. Only statistically significant variables were retained in the final reduced models through backward elimination to enhance model robustness and interpretability. Data visualization of the C/N ratio and glycerol content during bioreactor fermentation was performed using LabPlot software (Version 2.12.0).

Protein productivity was calculated as volumetric productivity (g/L/day in flasks; g/L/h in bioreactor runs) by dividing protein yield (g/L) by cultivation time. For Y4 in the RSM design, the maximum observed daily protein productivity was used. Protein yield was calculated from biomass concentration (g/L) multiplied by protein content.

3. RESULTS

3.1. Optimization of Medium by RSM

Thirty-one flask experiments were conducted using a central composite design, including unique and replicated medium compositions (Table 2).

Yeast growth dynamics were evaluated over a 5-day period, starting from the 3rd day of cultivation. The outcomes were categorized into three groups: no growth, moderate biomass accumulation, and high biomass accumulation. Absence of growth was observed in seven media formulations. The following parameters appeared critical for yeast inhibition: initial pH 3, 1.13 g/L urea at pH 7, 1.63 g/L urea at pH 6, and 2.13 g/L urea at pH 5. These results suggest a strong interaction between pH and urea concentration. Near-neutral pH values necessitate higher urea tolerance, whereas more acidic environments require lower urea content to avoid growth suppression. Moderate biomass accumulation was defined in the

range of 16.27–23.00 g/L, with maximum peak occurring on days 4, 5, or 7. High biomass accumulation was defined in the range of 27.60–34.77 g/L, with the maximum peak occurring on the 6th or 7th day of cultivation [22].

TABLE 2. EXPERIMENTAL MATRIX AND RESPONSE DATA FOR *P. RHODOZYMA* FERMENTATION

Run	Independent factors[1]				Responses[2]			
	A	B	C	D	Y1	Y2	Y3	Y4
1	75	1.63	3	4	22.10	22.53	0.042	1.24
2	75	0.63	7	6	22.23	24.18	0.041	1.34
3	75	0.63	7	4	17.30	25.78	0.054	1.11
4	90	1.13	5	5	23.20	22.36	0.036	1.30
5	90	1.13	5	5	25.20	22.67	0.040	1.43
6	90	1.13	5	7	0.20	–	–	–
7	90	0.13	5	5	17.83	28.58	0.059	1.27
8	75	1.63	3	6	0.90	–	–	–
9	90	1.13	1	5	23.37	24.36	0.045	1.42
10	75	0.63	3	6	23.30	25.47	0.048	1.48
11	105	1.63	7	4	22.00	22.27	0.041	1.22
12	120	1.13	5	5	23.90	23.87	0.040	1.43
13	75	0.63	3	4	17.67	26.40	0.055	1.17
14	105	1.63	7	6	0.77	–	–	–
15	90	1.13	5	3	−0.07*	–	–	–
16	90	1.13	5	5	24.10	25.82	0.040	1.56
17	90	1.13	5	5	25.03	22.09	0.039	1.38
18	90	1.13	9	5	22.63	20.98	0.040	1.19
19	75	1.63	7	6	0.37	–	–	–
20	105	0.63	7	6	22.80	23.24	0.042	1.32
21	105	0.63	7	4	16.27	24.22	0.053	0.99
22	105	0.63	3	6	23.83	22.53	0.047	1.34
23	60	1.13	5	5	22.20	22.76	0.037	1.26
24	90	1.13	5	5	24.60	21.69	0.036	1.33
25	105	1.63	3	6	0.40	–	–	–
26	75	1.63	7	4	22.03	22.09	0.041	1.22
27	90	1.13	5	5	23.80	22.71	0.034	1.35
28	105	0.63	3	4	15.77	25.69	0.054	1.01
29	105	1.63	3	4	22.57	24.00	0.045	1.35
30	90	2.13	5	5	1.70	–	–	–
31	90	1.13	5	5	22.20	25.6	0.040	1.42

[1] A: glycerol (g/L); B: CH_4N_2O (g/L); C: $(NH_4)_2SO_4$ (g/L); D: pH;
[2] Y1: biomass (g/L); Y2: protein content (%); Y3: astaxanthin content (%); Y4: protein productivity at the selected evaluation day (g/L/d).
* – value was ignored to improve the model.

Then, the biomass collected from triplicate cultures of the 24 medium formulations was analysed for protein and astaxanthin content in the biomass. The maximum protein values were reached on the 3rd day and gradually decreased over subsequent days of culture. The protein concentration in the biomass samples ranged from 25.24 % to 30.60 %. The maximum protein yield was reached typically on the 6th day and ranged from 4.29 g/L to 8.20 g/L. The maximum astaxanthin concentration was reached on the 6th or 7th day of cultivation and ranged from 0.046 % to 0.081 %. The maximum astaxanthin yield in the media supporting moderate and high biomass accumulation was 10.23–15.15 mg/L and 14.57–18.04 mg/L, respectively. In almost all samples, the productivity of protein was maximal on the 4th day of cultivation.

Protein productivity (g/L/day), a key parameter in SCP optimization, reached its maximum in the majority of experimental runs on day 4. For example, among the most productive conditions (e.g., runs 5, 10, 16, and 31), protein productivities exceeded 1.4–1.5 g/L/day on day 4, while corresponding values on days 5 to 7 either plateaued or declined. This indicates that day 4 marks the optimal balance point where biomass accumulation and protein biosynthesis intersect at their highest efficiency. Therefore, the 4th cultivation day was selected as the reference timepoint for RSM-based optimization, specifically due to the observed maxima in protein productivity, which is a critical factor for SCP-focused process development. Selecting a later time point (e.g., day 6 or 7) may have biased optimization towards higher biomass and astaxanthin at the expense of protein yield efficiency. Finally, for each medium, the response was evaluated using three criteria: biomass concentration (g/L), protein content (%), and astaxanthin content (%). However, only biomass and protein content were used as target variables for model optimization, while astaxanthin was considered a secondary trait and monitored for informational purposes.

Prior to optimization, the biomass data were subjected to a square root transformation to stabilize variance and enhance model interpretability. Subsequently, all models were refined through backward elimination, removing non-significant terms to improve model parsimony and predictive accuracy. Analysis of variance (ANOVA) confirmed that the second-order polynomial models (Table 3) were highly significant ($p < 0.0001$) and provided a robust fit for the relationship between the responses and the significant independent variables. All models demonstrated strong goodness-of-fit, with coefficients of determination (R^2) exceeding 0.9. The F-test results indicated that the models were statistically significant, with an extremely low probability (0.01 %) that the observed F-value could be attributed to noise. For all three responses, the observed F-values were substantially greater than the critical F-value at 0.05 for the corresponding degrees of freedom, confirming model adequacy and predictive significance. In addition, the lack-of-fit tests were non-significant ($p > 0.05$), indicating that the models adequately captured the experimental data without systematic deviation.

The final regression equations expressed in terms of coded factors (Table 4) were used to predict the response values of biomass yield, protein content, and astaxanthin concentration as functions of selected fermentation parameters. The use of coded models facilitates the comparison of the relative influence of each factor by standardizing their scales and enables the identification of key contributors to the modelled responses.

Among the four initially tested factors only urea (B) and pH (D) had a statistically significant impact on both biomass yield and protein content. In contrast, ammonium sulphate (C) showed statistical significance ($p < 0.001$) exclusively within the astaxanthin content model and was therefore excluded from the reduced models of biomass and protein yield. Similarly, glycerol (A) did not exert a statistically relevant effect on any of the three responses under the tested concentration range and was excluded from the reduced predictive models.

TABLE 3. ANOVA FOR THE SECOND-ORDER POLYNOMIAL MODELS

Response variable	Source	SS	DF	MS	F-value	p-value
Biomass	Model	74.14	5	14.83	1013.08	<0.0001
	Lack-of-fit	0.2797	18	0.0155	1.3	0.3947
	Pure error	0.0715	6	0.0119	–	–
	Total	74.49	29	–	–	–
	R^2	0.9953				
Protein content	Model	2391.99	5	478.4	312.68	<0.0001
	Lack-of-fit	17.87	17	1.05	0.3641	0.9529
	Pure error	17.32	6	2.89	–	–
	Total	2427.18	28	–	–	–
	R^2	0.9855				
Astaxanthin content	Model	0.0102	7	0.0015	405.23	<0.0001
	Lack-of-fit	0	16	2.621E-06	0.4267	0.9187
	Pure error	0	6	6.143E-06	–	–
	Total	0.0102	29	–	–	–
	R^2	0.9923				

SS – sum of squares; DF – degrees of freedom; MS – mean square

TABLE 4. FINAL EQUATIONS IN TERMS OF CODED FACTORS

	Biomass	Protein content	Astaxanthin content
Intercept	4.85	23.17	0.0382
B	−1.63	−13.65	−0.0286
C	–	–	−0.0024
D	−1.60	−12.20	−0.0262
BD	−4.65	−21.06	−0.0328
B^2	−2.12	−8.88	−0.0079
C^2	–	–	0.0051
D^2	−2.86	−11.71	−0.0105

A: glycerol (g/L); B: CH_4N_2O (g/L); C: $(NH_4)_2SO_4$ (g/L); D: pH

Urea and pH exhibited pronounced linear, interaction (BD), and quadratic effects, all characterized by negative coefficients. This indicates that deviations from their optimal range, whether lower or higher than optimal, have a detrimental impact on both biomass accumulation and protein synthesis. These findings support the presence of a well-defined optimal region within the experimental design space where moderate levels of urea and controlled pH favour microbial growth and protein biosynthesis.

The three-dimensional response surface plots Figs. 1(a)–(c) illustrate the interactive and nonlinear effects of selected medium components on *P. rhodozyma* biomass accumulation, protein and astaxanthin synthesis. The observed surface curvatures confirm the significance of both main and interaction effects identified in the regression models. In the case of biomass production Fig. 1(a), the response surface for urea and initial pH revealed a well-defined optimum within the studied range. The highest biomass yields were achieved at urea concentrations between 0.5 and 1.5 g/L, and pH values ranging from 4.0 to 6.5. Biomass formation declined sharply outside this range, supporting the presence of significant quadratic and interaction effects (particularly BD) in the model.

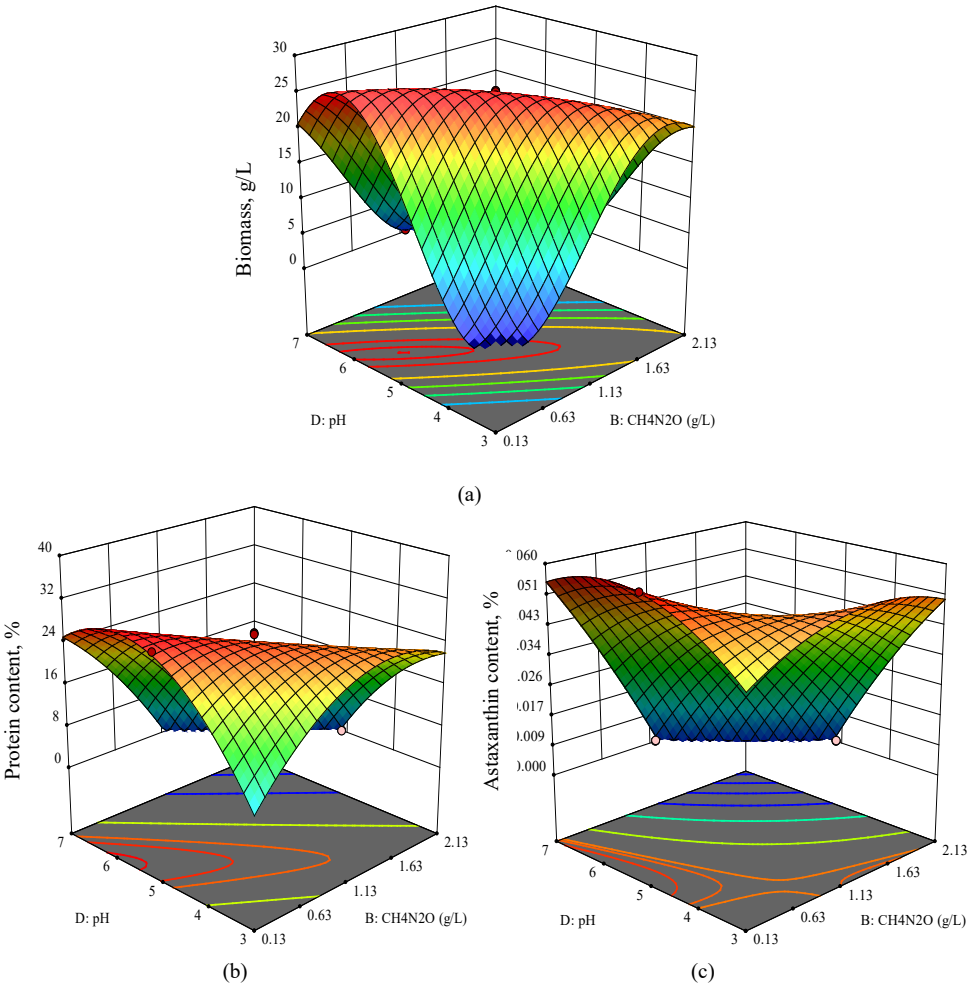


Fig. 1. The three-dimension response surface plots demonstrated the influence of the interaction between the two independent variables B and D on biomass (a), protein content (b), astaxanthin content (c).

Similarly, the surface plot for protein content Fig. 1(b) demonstrated that the most favourable conditions included urea concentrations between 0.13 and 0.8 g/L and pH values between 5.0 and 6.5. The narrow optimal region highlights the sensitivity of protein

accumulation to variations in nitrogen availability and pH, consistent with the negative curvature observed in the regression coefficients.

The response surface plot Fig. 1(c) illustrates the interactive effects of urea (CH_4N_2O) and initial pH on the astaxanthin content in *P. rhodozyma* biomass. The surface shows a pronounced central depression, forming a distinct saddle-shaped topology, which indicates a complex interaction between the two variables. The central depression in the astaxanthin surface further supports that pigment accumulation is favoured outside the growth and protein optimum, consistent with a metabolic shift away from primary biomass and protein synthesis under suboptimal nitrogen–pH combinations. Decreased astaxanthin content was observed at intermediate levels of both urea and pH, suggesting that neither factor alone was solely responsible for the increased pigment biosynthesis. Instead, low or high urea concentrations, as well as more acidic or alkaline pH conditions, resulted in increased astaxanthin production.

Although astaxanthin content was modelled as part of the experimental design, it was not included as an optimization target in this study. The primary objective was to maximize biomass yield and protein content, which were accordingly assigned goal importance values of +++ and +++++, respectively, within the optimization algorithm. Based on these criteria, numerical optimization using the desirability function approach identified three optimal formulations, each with a composite desirability score of 1, indicating the highest predicted alignment with target goals (Table 5). These solutions suggested moderate glycerol concentrations (70–90 g/L), low urea levels (<0.2 g/L), and slightly acidic pH (about 5.9) as favourable conditions for achieving simultaneous improvement in biomass and protein output.

TABLE 5. SHAKE-FLASK VALIDATION OF RSM-PREDICTED OPTIMAL MEDIA: PREDICTED VS EXPERIMENTAL RESPONSES (DAY 4 EVALUATION)

Medium No.	Variables				Predicted results			Experimental results		
	A	B	C	D	Y_1	Y_2	Y_3	Y_1	Y_2	Y_3
1	70.541	0.134	4.98	5.86	26.46	29.56	0.06	26.11	29.79	0.057
2	74.494	0.165	1.61	5.88	26.67	29.38	0.064	26.60	28.42	0.060
3	92.851	0.177	5.30	5.96	26.79	29.21	0.058	27.53	27.45	0.058

A: glycerol (g/L); B: CH_4N_2O (g/L); C: $(NH_4)_2SO_4$ (g/L); D: pH; Y_1: biomass yield (g/L); Y_2: protein content (%); Y_3: astaxanthin content (%)

The RSM-predicted optimal media were experimentally validated in independent triplicate shake-flask cultivations (Table 5), using the same day-4 response evaluation criterion applied in the optimization step. The experimental values closely matched the model predictions, confirming the robustness of the fitted models. Among the three optimized media, medium 1 (70.54 g/L glycerol, 0.134 g/L urea, 4.98 g/L ammonium sulphate, pH 5.86) was selected for scale-up due to its superior experimental performance in terms of protein accumulation and substrate conversion efficiency. Despite having the lowest total nitrogen input (1.12 g/L from urea and ammonium sulphate combined), Medium 1 supported a biomass yield of 26.11 g/L with a protein content of 29.79 %, corresponding to a protein concentration of 7.78 g/L. This resulted in a nitrogen-to-protein conversion efficiency exceeding 1:1, as the nitrogen recovered in biomass protein (1.24 g/L, assuming 16 % N content in protein) slightly exceeded the nitrogen supplied from the medium, indicating efficient nitrogen assimilation possibly supplemented by constant medium components.

The glycerol-to-biomass conversion ratio was approximately 0.37 g biomass per g glycerol, and glycerol-to-protein conversion reached 0.11 g protein per g glycerol, both of which were

superior to those achieved with the alternative media formulations. The moderate glycerol concentration (70.54 g/L) ensured balanced carbon availability without excess accumulation, thus reducing the risk of oxygen limitation or increased viscosity that could hinder large-scale fermentations and complicate downstream processing.

3.2. Batch Fermentation in Bioreactor

Optimized medium number 1 was successfully validated and selected for yeast cultivation in the 5 L bioreactor. The maximum biomass and protein concentrations were observed at 88 hours of cultivation, 33.50 g/L and 6.82 g/L (Table 6), which corresponds to the depletion of glycerol in the medium. After 88 hours, the biomass decreased, while the cell count continued to increase. The cumulative protein productivity increased over time, reaching a maximum of 0.092 g/L/h at 48 hours, after which it began to decline. These results suggest that the 48-h time point is optimal in terms of cumulative protein productivity under the tested conditions.

TABLE 6. BIOREACTOR FERMENTATION KINETICS

Time, h	Biomass, g/L	Cell concentration, cell/mL	Protein content, %	Protein yield, g/L	Protein productivity, g/L/h
0	1.07±0.50	8.60E+06	–	–	–
16	1.40±0.10	5.06E+07	40.18±3.00	0.56±0.04	0.035±0.003
25	2.87±0.23	1.08E+08	30.13±0.74	0.86±0.09	0.035±0.003
39	10.57±0.29	3.00E+08	24.89±0.20	2.63±0.05	0.067±0.001
48	20.60±0.46	3.42E+08	21.51±0.89	4.43±0.18	0.092±0.004
65	26.10±0.46	4.60E+08	20.27±1.83	5.29±0.41	0.081±0.006
72	28.80±0.78	4.74E+08	20.18±1.21	5.81±0.20	0.081±0.003
88	33.50±0.79	6.35E+08	20.36±0.73	6.82±0.12	0.078±0.001
97	31.60±0.85	6.45E+08	20.93±0.23	6.61±0.13	0.068±0.001
112	31.90±0.46	6.95E+08	20.87±0.28	6.67±0.22	0.059±0.002

The dynamic values of the C/N ratio and glycerol concentration during yeast cultivation in the bioreactor are shown in Fig. 2.

At the beginning of fermentation, the C/N ratio was approximately 26 with an initial glycerol concentration of 68.5 g/L, reflecting a high carbon loading relative to nitrogen. During the first 48 h of fermentation, glycerol gradually decreased to 41.2 g/L, while the C/N ratio increased to 29.9 at 39 h and remained elevated at 29.5 at 48 h. This increase in the C/N ratio suggests a relatively faster uptake of nitrogen compared to carbon during active biomass formation, as evidenced by the sharp increase in cell density and protein productivity during this phase. Between 48 and 88 h, glycerol was rapidly depleted, falling to 0 g/L, while the C/N ratio declined from 29.5 to 24.2. This phase marks a metabolic transition from nutrient-balanced growth to carbon-limited conditions. Despite the exhaustion of glycerol, the C/N ratio remained within a moderately narrow range (24–26) between 88 and 116 h, indicating that nitrogen assimilation had also slowed, consistent with entry into the stationary phase. The lowest C/N value was observed at 88 h, coinciding with the peak of biomass and protein yield.

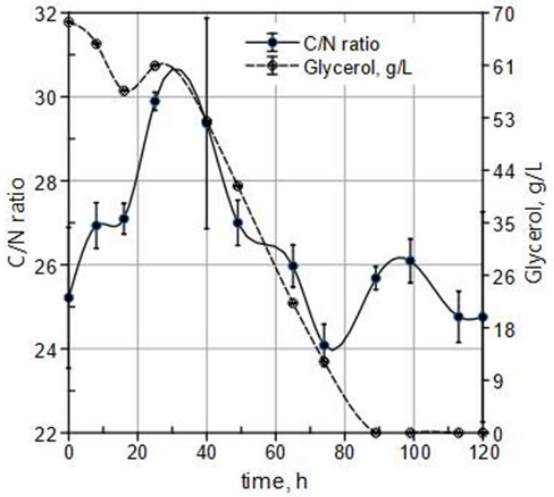


Fig. 2. Dynamics of C/N ratio and glycerol concentration during bioreactor cultivation of *P. rhodozyma* AEC3/9.

4. DISCUSSION

The present study demonstrates that *P. rhodozyma*, traditionally studied for astaxanthin biosynthesis, also holds promising potential as a SCP producer. In optimized conditions, biomass levels exceeding 26 g/L and protein concentrations up to 29.8 % in flask experiments. This protein fraction is on the lower end compared to many conventional SCP yeasts, for example, *Yarrowia lipolytica* contains 30–56 % protein [23], [24], *Saccharomyces cerevisiae* can reach about 45–50 % protein [25], [26], and *Candida* sp. about 39–60 % protein [27]–[30] under optimized culture conditions.

Despite this, the protein yield achieved by *P. rhodozyma* (up to 7.78 g/L in flask culture) is comparable to or higher than some SCP production reports with other yeasts on waste substrates. For instance, cultivation of *C. utilis* on capsicum waste yielded 6.8 g/L of SCP biomass [31], *C. guilliermondii* on sugar beet pulp produced 7.63 g/L protein [27], *Schwanniomyces etchellsii* on olive mill wastewater produced 5.42 g/L protein [28], and *Kluyveromyces marxianus* on cheese whey produced 6.14 g/L biomass [32]. Moreover, the biomass concentration of 26 g/L considerably exceeds earlier *P. rhodozyma* studies under suboptimal conditions (e.g. only 4.6 g/L biomass on peat hydrolysate medium, albeit with higher protein content about 47 % [33]. By comparison, our previous work [18] using organic nitrogen sources (yeast extract, peptone) achieved even higher biomass (~37 g/L) and protein yields (~12 g/L), highlighting that organic nitrogen can support greater protein productivity. Future studies could explore replacing costly organic nitrogen with food by-products or waste streams to combine high yields with economic and environmental benefits.

A key outcome of the CCD/RSM analysis was that urea concentration and initial pH, dominated biomass and protein responses within the studied design space. This suggests that, under the tested carbon-excess conditions (60–120 g/L glycerol), nitrogen availability and acid-base balance were more limiting for SCP formation than total carbon supply. Beyond compositional optimization, Medium 1 demonstrated several process-friendly characteristics. Its low nitrogen loading (1.12 g/L) effectively supported high biomass and protein yields while minimizing risks of ammonium toxicity and foam formation – two common issues in

high-cell-density bioreactors [34]. The pH of 5.86 proved optimal for yeast growth while providing a buffer window for future pH-shift induction strategies to promote astaxanthin biosynthesis [35]. Importantly, even though astaxanthin synthesis was not directly targeted in this study, all optimized flask runs yielded measurable pigment levels, indicating that SCP-focused media do not completely inhibit carotenoid synthesis, thereby supporting the dual-value proposition of *P. rhodozyma* biomass. This context of results in flasks provides a foundation for interpreting bioreactor experiments, where process dynamics and scalability become critical.

Temporal C/N ratio dynamics in bioreactor experiments further confirmed metabolic phase transitions. A rising C/N value during early exponential growth reflected rapid nitrogen assimilation, while the subsequent decline, despite glycerol exhaustion, indicated a shift into stationary-phase metabolism. These observations confirm that the C/N ratio serves as a valuable real-time indicator of the physiological state of the culture. Our data suggest that targeted glycerol feeding between 74–89 h could further extend biomass accumulation and protein biosynthesis, thereby increasing overall process productivity. This supports the rationale for fed-batch implementation strategies [36], where controlled C/N management can delay metabolic slowdown and sustain favourable SCP production kinetics.

From a commercial standpoint, the optimized *P. rhodozyma* SCP process shows promise, especially for aquaculture and animal feed applications. The SCP yields and product composition achieved are within a viable range for industrial fermentation, and the use of glycerol as carbon source positions the process well for integration with biodiesel or oleochemical industries where glycerol is an abundant, low-cost by-product. Converting waste glycerol to high-protein yeast biomass embodies a circular economy approach, reducing waste and producing feed protein – a strategy echoed by recent studies on SCP from various residues [37], [38]. A techno-economic analysis on a similar red yeast (*Rhodotorula glutinis*) process using food industry residues estimated a production cost of $1308/ton SCP which could drop to $762/ton with nutrient cost optimizations [39]. These figures suggest that microbial protein with co-products can be produced at costs on the same order as conventional soybean meal or fish meal, especially when pigmented SCP might justify a higher price. *P. rhodozyma* SCP specifically could target niches where its astaxanthin content adds value, for example, inclusion in salmonid diets not only provides protein but also contributes pigmentation. Feeding trials reported in the literature have already demonstrated the effectiveness of *P. rhodozyma* as a pigment source in salmonid diets, and regulatory authorities have assessed the safety of astaxanthin-enriched yeast for use in animal feeds [40]. This indicates a path to market already exists, and our work on optimizing SCP production improves the efficiency of generating such a product.

5. CONCLUSION

The optimisation of *P. rhodozyma* SCP production via RSM has yielded moderate amounts of single-cell protein, characterised by the unique feature of concurrent astaxanthin production. Response surface methodology successfully identified a low-cost glycerol medium region for *P. rhodozyma* AEC3/9 cultivation, with urea concentration and initial pH as the dominant factors affecting biomass and protein responses. The optimal formulation (70.54 g/L glycerol, 0.134 g/L urea, 4.98 g/L $(NH_4)_2SO_4$, pH 5.86) was validated in shake flasks and produced 26.11 g/L biomass with 29.79 % protein (7.78 g/L protein), while astaxanthin remained detectable as a non-target co-product. Scale-up in a 5 L bioreactor confirmed process feasibility, reaching 33.50 g/L biomass and 6.82 g/L protein at 88 h, and showed that maximal protein productivity occurred earlier than maximal biomass

accumulation. The study supports *P. rhodozyma* as a dual-purpose platform for SCP and astaxanthin co-production and provides a statistical basis for further process intensification, including fed-batch cultivation and low-cost waste-derived substrates. The protein yield and productivity represent an improvement over previously reported *P. rhodozyma* batch cultivations. While there remains a gap between *P. rhodozyma* and the most efficient yeast SCP systems, this gap is partially bridged by the multi-product output. Process co-produces astaxanthin, conferring added value that can offset some of the lesser protein density. Astaxanthin-rich SCP offers functional benefits that conventional SCP lacks. With further enhancements – such as fed-batch strategies, waste feedstocks, and strain improvements – the process could become more competitive in terms of pure protein metrics as well. *P. rhodozyma* SCP production can be a viable component of sustainable protein sourcing for animal diets, particularly for aquaculture, where its intrinsic astaxanthin offers a market advantage. The concept of integrating SCP production with waste valorization and simultaneously harvesting a value-added astaxanthin a modern biorefinery approach that could improve economic feasibility.

DATA AVAILABILITY

Raita S, Kuzmika I, Geiba Z, Kusnere Z, Palcevska J. Experimental dataset on biomass, protein, and astaxanthin production by the mutant yeast *Phaffia rhodozyma* AEC3/9 in flask and bioreactor cultivation. Zenodo link: https://doi.org/10.5281/zenodo.18981853

ACKNOWLEDGEMENT

This work was supported by the Fundamental and Applied Research Project "Herbicides as a tool for selection of edible protein-rich mutants", project No. lzp-2022/1-0126, funded by the Latvian Council of Science.

REFERENCES

[1] Lähteenmäki-Uutela A., Rahikainen M., Lonkila A., Yang B. Alternative proteins and EU food law. *Food Control* 2021:130:108336. https://doi.org/10.1016/j.foodcont.2021.108336

[2] Margareth O., Anders S. Yeast derived from lignocellulosic biomass as a sustainable feed resource for use in aquaculture. *Journal of the Science of Food and Agriculture* 2016:97(3):733–742. https://doi.org/10.1002/jsfa.8007

[3] Oliva-Teles A., Guedes M. J., Vachot C., Kaushik S. J. The effect of nucleic acids on growth, ureagenesis and nitrogen excretion of gilthead sea bream *Sparus aurata* juveniles. *Aquaculture* 2006:253(1–4):608–617. https://doi.org/10.1016/j.aquaculture.2005.09.010

[4] Grammes F., Reveco F. E., Romarheim O. H., Landsverk T., Mydland L. T., Øverland M. *Candida utilis* and *Chlorella vulgaris* counteract intestinal inflammation in Atlantic salmon (*Salmo salar* L.). *PLoS ONE* 2013:8(12). https://doi.org/10.1371/journal.pone.0083213

[5] Lall S. P., Anderson S. Amino acid nutrition of salmonids: dietary requirements and bioavailability. *Cahiers Options Méditerranéennes* 2005:63:73–90.

[6] Sharif M., Zafar M. H., Aqib A. I., Saeed M., Farag M. R., Alagawany M. Single cell protein: Sources, mechanism of production, nutritional value and its uses in aquaculture nutrition. *Aquaculture* 2021:531. https://doi.org/10.1016/j.aquaculture.2020.735885

[7] Bratosin B. C., Darjan S., Vodnar D. C. Single cell protein: A potential substitute in human and animal nutrition. *Sustainability (Switzerland)* 2021:13(16):1–24. https://doi.org/10.3390/su13169284

[8] Jannathulla R., Sravanthi O., Moomeen S., Gopikrishna G., Dayal J. S. Microbial products in terms of isolates, whole-cell biomass, and live organisms as aquafeed ingredients: production, nutritional values, and market potential—a review. *Aquaculture International* 2021:29:623–650. https://doi.org/10.1007/s10499-021-00644-2

[9] Aas T. S., Grisdale-Helland B., Terjesen B. F., Helland S. J. Improved growth and nutrient utilisation in Atlantic salmon (*Salmo salar*) fed diets containing a bacterial protein meal. *Aquaculture* 2006:119(2):300–315. https://doi.org/10.1016/j.aquaculture.2006.05.032

[10] Li P., Gatlin D. M. Nucleotide nutrition in fish: Current knowledge and future applications. *Aquaculture* 2006:251(2–4):141–152. https://doi.org/10.1016/j.aquaculture.2005.01.009

[11] Glencross B. D., Huyben D., Schrama J. W. The Application of Single-Cell Ingredients in Aquaculture Feeds—A Review. *Fishes* 2020:5(3):22. https://doi.org/10.3390/fishes5030022

[12] Marius K. S. *et al.* Optimization of *Saccharomyces cerevisiae* SKM10 single cell protein production from mango (*Magnifera indica* L.) waste using response surface methodology. *African Journal of Biotechnology* 2017:16(45):2127–2133. https://doi.org/10.5897/AJB2017.16210

[13] Tabssum F., Irfan M., Shakir H. A., Qazi J. I. RSM based optimization of nutritional conditions for cellulase mediated Saccharification by *Bacillus cereus*. *J Biol Eng* 2018:12(1):7. https://doi.org/10.1186/s13036-018-0097-4

[14] Bardhan P., Baruah J., Raj G. V. S. B., Kalita E., Mandal M. Optimization of culture conditions for biomass and lipid production by oleaginous fungus Penicillium citrinum PKB20 using response surface methodology (RSM). *Biocatalysis and Agricultural Biotechnology* 2021:37:102169. https://doi.org/10.1016/j.bcab.2021.102169

[15] Beigbeder J.-B., De Medeiros Dantas J. M., Lavoie J.-M. Optimization of Yeast, Sugar and Nutrient Concentrations for High Ethanol Production Rate Using Industrial Sugar Beet Molasses and Response Surface Methodology. *Fermentation* 2021:7(2):86. https://doi.org/10.3390/fermentation7020086

[16] Hawaz E. *et al.* Optimization of bioethanol production from sugarcane molasses by the response surface methodology using *Meyerozyma caribbica* isolate MJTm3. *Ann Microbiol* 2023:73(1):2. https://doi.org/10.1186/s13213-022-01706-3

[17] Roberts T. M., Kaltenbach H., Rudolf F. Development and optimisation of a defined high cell density yeast medium. *Yeast* 2020:37(5–6):336–347. https://doi.org/10.1002/yea.3464

[18] Raita S., Kuzmika I., Mika T., Geiba Z., Spalvins K. Enhanced amino acid biosynthesis in *Phaffia rhodozyma* via herbicide-induced selection. *Journal of Industrial Microbiology and Biotechnology* 2025:52:kuaf011. https://doi.org/10.1093/jimb/kuaf011

[19] Guerlava P., Izac V., Tholozan J. L. Comparison of different methods of cell lysis and protein measurements in *Clostridium perfringens*: Application to the cell volume determination. *Current Microbiology* 1998:36(3):131–135. https://doi.org/10.1007/PL00006756

[20] Luna-Flores C. H., Wang A., von Hellens J., Speight R. E. Towards commercial levels of astaxanthin production in *Phaffia rhodozyma*. *Journal of Biotechnology* 2022:350:42–54. https://doi.org/10.1016/j.jbiotec.2022.04.001

[21] Ni H., He G. Q., Ruan H., Chen Q. H., Chen F. Application of derivative ratio spectrophotometry for determination of β-carotene and astaxanthin from *Phaffia rhodozyma* extract. *Journal of Zhejiang University: Science* 2005:6:514–522. https://doi.org/10.1631/jzus.2005.B0514

[22] Raita, S., Kuzmika I., Geiba Z., Kusnere Z., Jelizaveta P. Experimental dataset on biomass, protein, and astaxanthin production by the mutant yeast *Phaffia rhodozyma* AEC3/9 in flask and bioreactor cultivation. *Zenodo* 2026. https://doi.org/10.5281/zenodo.18981853

[23] Rages A. A., Haider M. M., Aydin M. Alkaline hydrolysis of olive fruits wastes for the production of single cell protein by *Candida lipolytica. Biocatalysis and Agricultural Biotechnology* 2021:33:1–6. https://doi.org/10.1016/j.bcab.2021.101999

[24] Jach M. E., Malm A. Yarrowia lipolytica as an Alternative and Valuable Source of Nutritional and Bioactive Compounds for Humans. *Molecules* 2022:27(7):2300. https://doi.org/10.3390/molecules27072300

[25] Michalik B., Biel W., Lubowicki R., Jacyno E. Chemical composition and biological value of proteins of the yeast *Yarrowia lipolytica* growing on industrial glycerol. *Canadian Journal of Animal Science* 2014:94(1):99–104. https://doi.org/10.4141/cjas2013-052

[26] Hezarjaribi M., Ardestani F., Ghorbani H. R. Single Cell Protein Production by *Saccharomyces cerevisiae* Using an Optimized Culture Medium Composition in a Batch Submerged Bioprocess. *Applied Biochemistry and Biotechnology* 2016:179(8):1336–1345. https://doi.org/10.1007/s12010-016-2069-9

[27] Patelski P. *et al.* Utilisation of sugar beet bagasse for the biosynthesis of yeast SCP. *Journal of Food Engineering*, 2015:167:32–37. https://doi.org/10.1016/j.jfoodeng.2015.03.031

[28] Arous F., Azabou S., Jaouani A., Zouari-Mechichi H., Nasri M., Mechichi T. Biosynthesis of single-cell biomass from olive mill wastewater by newly isolated yeasts. *Environmental Science and Pollution Research* 2016:23(7):6783–6792. https://doi.org/10.1007/s11356-015-5924-2

[29] Kurcz A., Błażejak S., Kot A. M., Bzducha-Wróbel A., Kieliszek M. Application of Industrial Wastes for the Production of Microbial Single-Cell Protein by Fodder Yeast *Candida utilis. Waste and Biomass Valorization* 2018:9(1):57–64. https://doi.org/10.1007/s12649-016-9782-z

[30] Magalhães C. E. B., Souza-Neto M. S., Astolfi-Filho S., Matos I. T. S. R. *Candida tropicalis* able to produce yeast single cell protein using sugarcane bagasse hemicellulosic hydrolysate as carbon source. *Biotechnology Research and Innovation* 2018:2(1):19–21. https://doi.org/10.1016/j.biori.2018.08.002

[31] Zhao G., Zhang W., Zhang G. Production of single cell protein using waste capsicum powder produced during capsanthin extraction. *Letters in Applied Microbiology* 2010:50(2):187–191. https://doi.org/10.1111/j.1472-765X.2009.02773.x

[32] Koukoumaki D. I., Papanikolaou S., Ioannou Z., Mourtzinos I., Sarris D. Single-Cell Protein and Ethanol Production of a Newly Isolated *Kluyveromyces marxianus* Strain through Cheese Whey Valorization. *Foods* 2024:13(12):1892. https://doi.org/10.3390/foods13121892

[33] Martin A. M., Acheampong E., Patel T. R. Production of astaxanthin by *Phaffia rhodozyma* using peat hydrolysates as substrate. *Journal of Chemical Technology & Biotechnology*. 1993:58(3):223–230. https://doi.org/10.1002/jctb.280580304

[34] Tiso T. *et al.* Foam control in biotechnological processes—challenges and opportunities. *Discov Chem Eng* 2024:4(1):2. https://doi.org/10.1007/s43938-023-00039-0

[35] Kanwugu O. N., Shatunova S. A., Glukhareva T. V., Kovaleva E. G. Effect of different sugar sources on *P. rhodozyma* Y1654 growth and astaxanthin production. *Agronomy Research* 2020:18(3). https://doi.org/10.15159/AR.20.117

[36] Pan D. *et al.* Homologous High-Level Lipase and Single-Cell Protein Production with Engineered *Yarrowia lipolytica* via Scale-Up Fermentation for Industrial Applications. *Fermentation* 2023:9(3):268. https://doi.org/10.3390/fermentation9030268

[37] Pereira A. G. *et al.* Single-Cell Proteins Obtained by Circular Economy Intended as a Feed Ingredient in Aquaculture. *Foods* 2022:11(18):2831. https://doi.org/10.3390/foods11182831

[38] Guo T., Bode J., Kuka K., Tippkötter N. Enhancing Single-Cell Protein Yield Through Grass-Based Substrates: A Study of *Lolium perenne* and *Kluyveromyces marxianus*. *Fermentation* 2025:11(5):266. https://doi.org/10.3390/fermentation11050266

[39] Li Y. *et al.* Production of single-cell protein from vinegar residue by *Rhodotorula glutinis* and techno-economic analysis. *Bioresource Technology* 2025:422:132252. https://doi.org/10.1016/j.biortech.2025.132252

[40] Zantioti C., Dimitroglou A., Mountzouris K. C., Miliou H., Malandrakis E. E. Use of pigmented fungi as additives in aquaculture. *Aquacult Int* 2025:33(3):162. https://doi.org/10.1007/s10499-025-01840-0